POAC'23
Glasgow, United Kingdom

Proceedings of the 27th International Conference on
Port and Ocean Engineering under Arctic Conditions
12-16 June 2023, Glasgow, UK

Caspian Deformed Ice Cover Classification

Yevgeniy Kadranov[1], Sergey Vernyayev[1], Anton Sigitov[1]
[1] ICEMAN.KZ LLP (Almaty, Kazakhstan)

ABSTRACT

Deformed ice is a general term for ice which has been squeezed together and in places forced upwards (and downwards). Subdivisions are rafted ice, ridged ice and hummocked ice. There are little to no physical observations available for the Caspian Sea region. Specifically, there is little knowledge available on spatial and temporal distribution of ice ridges. Nevertheless, these features are critical and have significant impact both on design of structures and planning marine operations. This article introduces results of unsupervised classification of SAR data using k-means algorithm that allows for automatic detection and segmentation of areas with low medium and high backscatter level that define degree of deformation. The method was used to interpret imagery archives for an area in the Northeastern part of the sea. Compiled time series was interpolated based on ice movement events records to ensure consistent and analyzable record. The dataset was used to derive descriptive statistics illustrating frequency of phenomena occurrence and distributions of intensity spatially and through the observations period.

KEY WORDS: Caspian Sea; Deformed ice; Ice ridges distribution; Regional ice monitoring; SAR images classification.

NOMENCLATURE
SAR (Synthetic Aperture Radar) FDD (Freezing Degree Days)

INTRODUCTION

The Caspian Sea is the largest enclosed body of water on Earth and plays a critical role in the socio-economic and environmental well-being of the surrounding countries. During winter, the Caspian Sea is subject to cold weather conditions, leading to the formation of ice cover that can significantly affect offshore activities. Accurate and timely monitoring of ice cover is, therefore, essential for managing and mitigating associated hazards. As opposed to other economically active ice-covered areas there are little to no publicly available quality ice cover data sources. The need for ice cover related information and analysis is satisfied within scope of commercial projects supporting specific operations like shipping through Volga-Caspian Channel or operations support of oil and gas fields development and exploitation.

Internal ICEMAN.KZ project on compiling an overwhelming ice database for the Northern

Caspian area is a change to the situation. Caspian Sea Ice Cover Hindcast Database by Vernyayev et al. (2023a) is the basis containing detailed information on ice cover and metocean conditions as observed during the recent history in 2000s. Ice drift records describing the rate of mobile ice cover displacements (Kadranov et al., 2017) and stamukhi database comprising the record of the ice feature distribution across the region (Sigitov et al., 2019) are add-on to the database. This paper introduces deformed ice coverage spatiotemporal distribution component that closes the gap in data records by features of interest for support of offshore activities.

Deformed ice is a general term for ice which has been squeezed together and in places forced upwards (and downwards). Subdivisions are rafted ice, ridged ice and hummocked ice (Canadian Ice Service, 2005). Figure 1 shows the variety of deformed ice features that are focused on in this study's interest area. The key distinction is significantly rougher surface with a lot of sharp edges and irregularities.

These features are normally thicker than the ambient ice cover, including mainly level ice. Thus, they pose higher hazard to offshore structures and operations. To which degree interactions with deformed ice are more hazardous has always been a matter of discussion. For fixed structures it is a combination of drift events and number of ridges or encounters with more severe features. For marine vessels forming conventional ice breaking fleet it is the frequency of ridges that they encounter during transit and effect on speed and travel time. For air cushion vehicles it is the spatial coverage of the area they pass through that is rough surface and covered with high sails that damage skirts and lead to downtime ashore to fix the damage. These are only some of the challenges that are encountered in offshore operations where reliable and unbiased observations of ridged ice distribution are a requirement to derive quantified impact assessment (Eicken and Mahoney, 2015).

Note stamukhi as a grounded ice rubble feature being the terminal stage of ice cover deformation and typical features for the Northern Caspian are not considered with this study forming the exclusion. They comprise a separate segment of monitoring program as described by Sigitov et al. (2019) due to different applications and detection methodology.

Figure 1 Photos of deformed ice as observed in the Caspian Sea illustrating rough surface of ice cover.

WMO (2014) suggests a single point symbol indicates presence of ice ridges with linear density per 1 km. This definition was the center point that most observation programs we have encountered are based on. Attempt to statistically analyze datasets (either symbols on ice charts or journal records in transit reports) collected with this approach has always led to more discussions on how biased the observations are, how to cope with irregularity. But the result was always a qualitative description of event observations.

In our search for an unbiased way to compile deformed ice coverage dataset we have deviated from the traditional ice charting approach. We have used remote sensing technologies instead.

Or to be more specific we rely on Synthetic Aperture Radar (SAR) that is regular, independent of weather and has significant coverage. SAR data can provide information on the backscattering properties of ice cover (Sandven et al., 2006), which can be used to distinguish ice types. Karvonen (2012), Linow et al. (2015), Scheuchl et al. (2001) discuss similar work and associated SAR data interpretation.

This paper illustrates how this technology was applied to a focus area around Kashagan oil field in the Caspian Sea where demand for ice related analysis is the highest in the region due to intensive operations and continued field development efforts. Most importantly the focus of SAR data interpretation was targeted on creation of timeseries of comparable and analyzable data to track trends for multiple days and seasons. Some of the resulting insights on deformed ice occurrence illustrate practical meaning of data to support operational planning and engineering.

DATA PROCESSING

Source Data and Classification Algorithm

K-means clustering (Lloyd, 1982) algorithm was applied to SAR data acquired with the Sentinel-1 satellite to find and classify several types of ice cover over specific areas in the region as a method of area classification by severity of deformation. The time series of classification were derived from the same platform for both A and B busses until the loss of the latter from the beginning of the mission in 2014 to 2022.

K-means is unsupervised machine learning algorithm that partitions the given data (in our case backscatter level of satellite image) into predefined number (k) of clusters. The algorithm iteratively partitions an image into clusters by minimizing variance within cluster. This algorithm was chosen as it has low computational cost and does not require large and labeled dataset.

Specifically for this dataset, three distinct types of deformed ice were considered:

(1) Definitely deformed ice including ice ridges refrozen navigation channels and other features with high top surface roughness,
(2) Semi deformed ice cover consisting of mixed by coverage flat ice and deformed ice, and (3) flat level ice or open water.

The backscatter value in each pixel of a SAR image defines the degree of ice cover deformation through surface roughness. Deformed ice with high coverage and high roughness gives the most intensive backscatter. It allowed for automatic detection and segmentation of areas with low medium and high deformation.

Figure 2 illustrates a typical histogram of a sample SAR scene's clustered backscatter signal illustrating distribution of the three deformed ice categories in one observation.

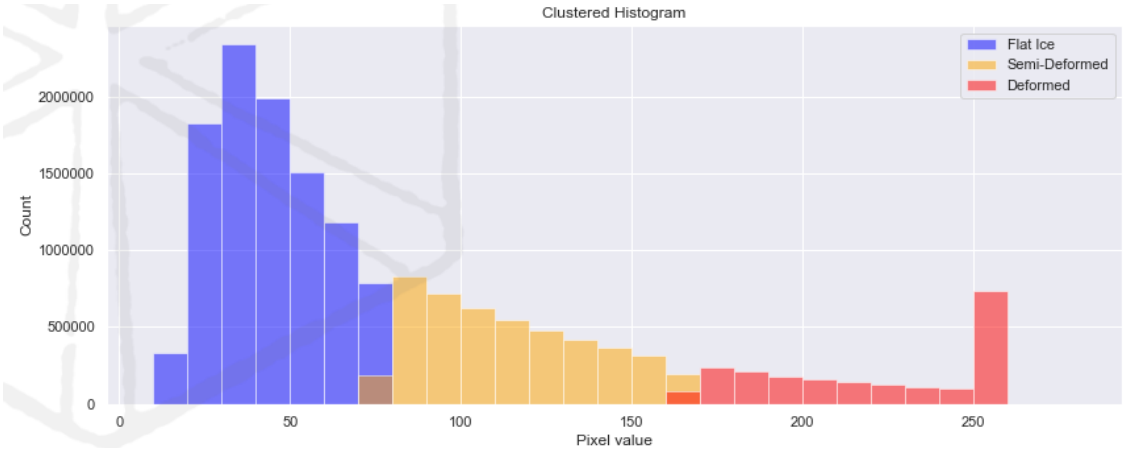

Figure 2 Clustered histogram of backscatter signal acquired with Sentinel-1 image 13 January 2015.

Algorithm Validation and Resolution of Ambiguities

Several experiments with normal unsupervised remote sensing data interpretation have shown inability of the algorithm to distinguish:

- Heavily ridged areas and open water leads or water within low concentration under windy conditions due to high backscatter from Bragg waves (Phillips, 1988) on water surface. This is a known issue of automated SAR data interpretation for sea ice analysis purposes.
- Flat ice, open water leads, or water within low concentration under calm wind conditions or still.
- Heavily ridged areas and navigation channels.

The ambiguities in the automated classification of SAR backscatter data were resolved with more spatial conditional filters to remove mistaken data from the final dataset. Lohse et al. (2020) presents a more detailed discussion on complexity of continuous sea ice monitoring programs and methods used to resolve them.

Issue with Bragg waves that form on surface of open water leads forming during drift events or break-up was resolved with removing clustered classification values based on coincidence with opening leads and areas of low concentration from ice cover classification data by Vernyayev et al. (2023a). The dataset is detailed enough to distinguish from the surrounding ice cover of higher concentration. Remaining areas with ice concentration 9/10 or above and omitting areas with ice that is significantly thinner than surrounding area ice thickness. The same filter removed flat ice and smooth water surface during still with flat ice areas with water nilas and new ice formations. This filter cuts off days and areas with low ice concentration and newly formed leads resetting deformed ice coverage to zero. This corresponds to reality with opening leads because normally they are covered with high concentrations of either nilas under calm conditions, or pancake ice with strong wind, given air temperature is low enough to ensure refreezing. Either way significant deformed ice features with deep keels are limited.

The issue with classification of navigation channels as heavily deformed areas was not resolved. However, from the statistical point of view the area covered with channels is negligibly minor compared to the area of ice ridge network developing over the region from one hand. From the other, normally collapsing heavily navigated channels form an ice ridge with rubble pushed under the sheet ice forming a keel. So, channels may be considered as a potential ridge.

Figure 3 shows the sample image (left) and classification result (right). Note the pre-coastal area was excluded from analysis with mask to account for water level variation between seasons and wind induced surges during seasons. This mask removed uncertainties associated with land detection. The same mask includes Kashagan offshore structures with rationale to remove disturbance in each image that is caused by high backscatter from steel structures, rock and rubble that piles up at faces of the islands in the well-developed field.

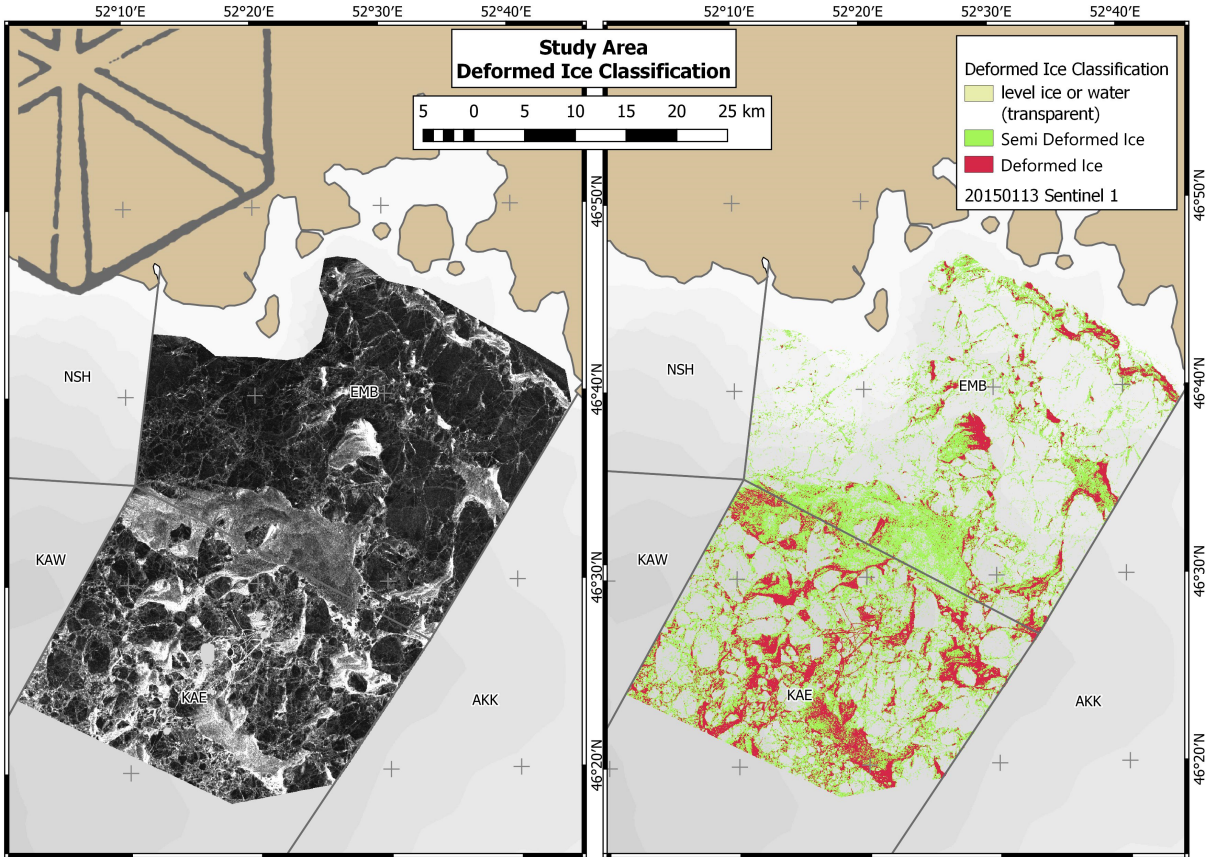

Figure 3. Original (left) and clustered (right) Sentinel-1 image from 13 January 2015 where categories 1 and 2 illustrate two distinct types of deformed ice cover.

Timeseries Compilation

Sentinel-1 data (ESA, 2014-2023) was used to derive timeseries of deformed ice observations over the area of interest as it forms the longest consistent dataset in the region that is available with free access. To ensure classification results are comparable between images through a season and the history of all years of available years, specific orbits were picked with full coverage of the study area. Overall, 104 images were processed for all seasons from 2014 to 2022. On average 7 days between each observation have formed gaps in observations. Resulting pixel values were summarized into a 1×1 km grid as area coverage by category of deformed ice.

Considering most analysis applications developed in house are based on data with daily frequency interpolation to reduce gap between observations was considered a solution to regularize the dataset and make it compatible with other data sources. The following logic was applied to ensure ice cover evolution and key ice events that lead to redistribution of ice masses in the area are considered:

- If grid cell was in immobile conditions based on mobility data from Vernyayev et al. (2023a) following the observation, observed deformation values were propagated until the next observation or days with mobile conditions. The logic is that if ice did not move there was no energy in the ice sheet to cause deformation.
- If mobile or open water conditions were observed between two images followed by immobile conditions deformed ice values for days with immobile conditions are substituted with next observation. If deformation took place, it was when ice moved not when it was recorded immobile.
- Mobile conditions with daily mean wind speed below 10 knots were considered immobile and interpolation rules were applied as above.
- If there was a noticeable thickness reduction (10 cm less than previous day) between observations, then the cover of deformed and semi deformed ice was set to zero as the reduction indicated a lead that has opened and refroze.
- If mobile ice with concentration above 5/10 and compacting, then the next observation is assigned as it shows consequences of an ice event that occurred during the day of compaction or drifting ice with increasing concentration.

Resulting interpolated daily dataset of deformed ice coverage by two categories (deformed and semi deformed) was thus compiled into a grid with 1×1 km cell size. The dataset is consistent through the study area and without gaps in time. It is also consistent with other databases like ice cover classification from hindcast, aggregated metocean records and ice drift as visualized with Figure 4 below for one of the seasons. Referenced databases contain more details about the parameters displayed. This compatibility enables cross correlation of various parameters to describe cause and effect for most ice phenomena or interactions with vessels or fixed structures.

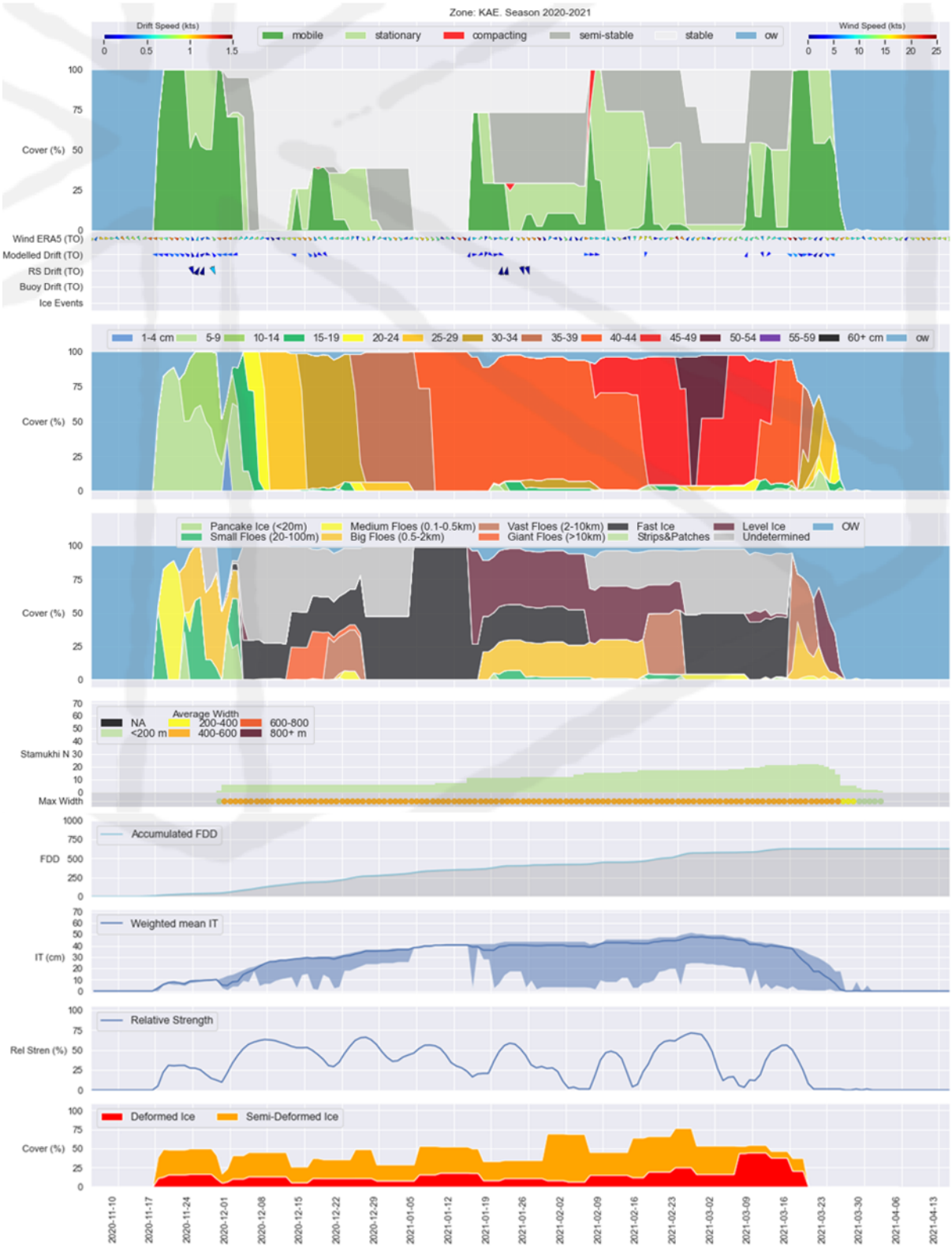

Figure 4 One season of combined ice and metocean parameters as observed during a season in a zone of the study area.

RESULTING INSIGHTS

The most obvious advantage of compiling deformed ice information with this approach is that spatial analysis of phenomena distribution over an area becomes straight forward and unbiased to human interpretation of standard WMO symbology for ridges. Figure 5 illustrates spatial distribution of annual frequency of deformed and semi deformed ice coverage occurrence for the period of available data from 2014 to 2022 over each 1×1 km grid cell in the study area. Interpolated data and observations were normalized by duration of season from November 01 to April 15 to make distributions comparable between seasons.

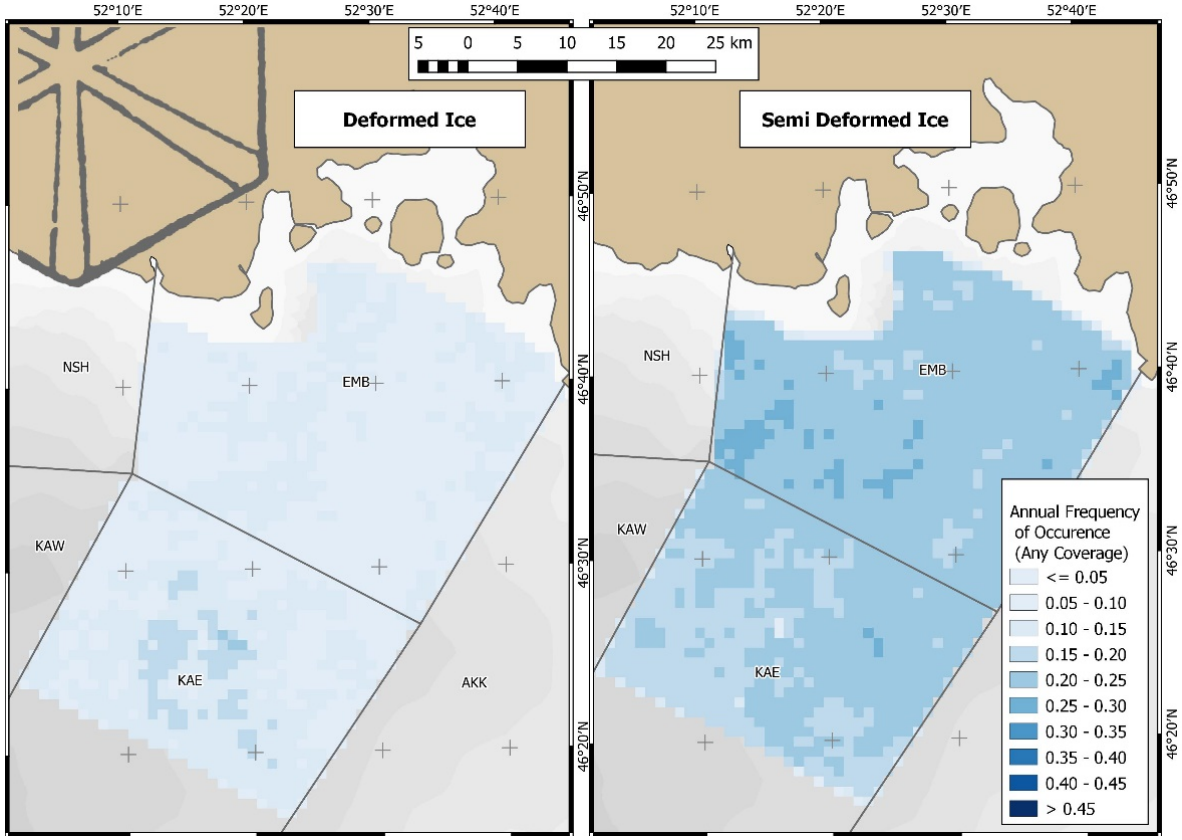

Figure 5 Annual frequency of deformed ice (left) and semi deformed ice (right) coverage occurrence for period from 2014 to 2022 with seasons normalized by duration from November 01 to April 15.

This presentation enabled quantified identification of areas with higher occurrence rate of deformed ice. In this case darker semi deformed ice areas halfway from Kashagan to the Northern coast identify the area of recurring interface of normally fast ice and mobile ice cover. This observation was confirmed with knowledge database of ice charting operators that have recorded the area as a high potential for ridge and stamukhi formation based on daily observations they have recorded for hindcast database. Higher frequency of deformed ice around structures at Kashagan is also informative as it confirms the theory of higher ridge frequency occurring near fixed structures.

Building Interaction Scenarios and Supporting Operations

Either of the dataset's components enable practical analysis of operations. For example, when planning air cushion vehicle (ACV) operations such parameters as transit route and travel time

can now be closer to reality replacing straight lines with curves avoiding areas that were observed deformed more often than the others. As the phenomena seems to be recuring season-to-season further optimization of ACV usage can be achieved through, as example, best position of shore station to minimize routes outside of rough ice conditions and thus reduction of downtime due to skirts repair (Kadranov et al., 2023).

Same type of spatial analysis can be performed for any operation or structure design with known response and sensitive to presence of deformed ice. Considering duration of deformed ice presence and most importantly persistence and intensity of its presence in each square kilometer of the study area quantified impact assessment becomes a matter of defining scenario of interaction. The latter defines an algorithm to assess events that a subject for analysis could have experienced adverse conditions. As such analysis is performed for the whole study area simultaneously as illustrated with the figure below a sensitivity map is created to define areas with favorable and unfavorable conditions. Figure 6 shows scenarios can be built differentially in terms of tolerance to spatial coverage by deformed ice and with consideration to other indices. For illustration purposes the two categories of deformed ice with various coverage were presented for random mild and moderate seasons.

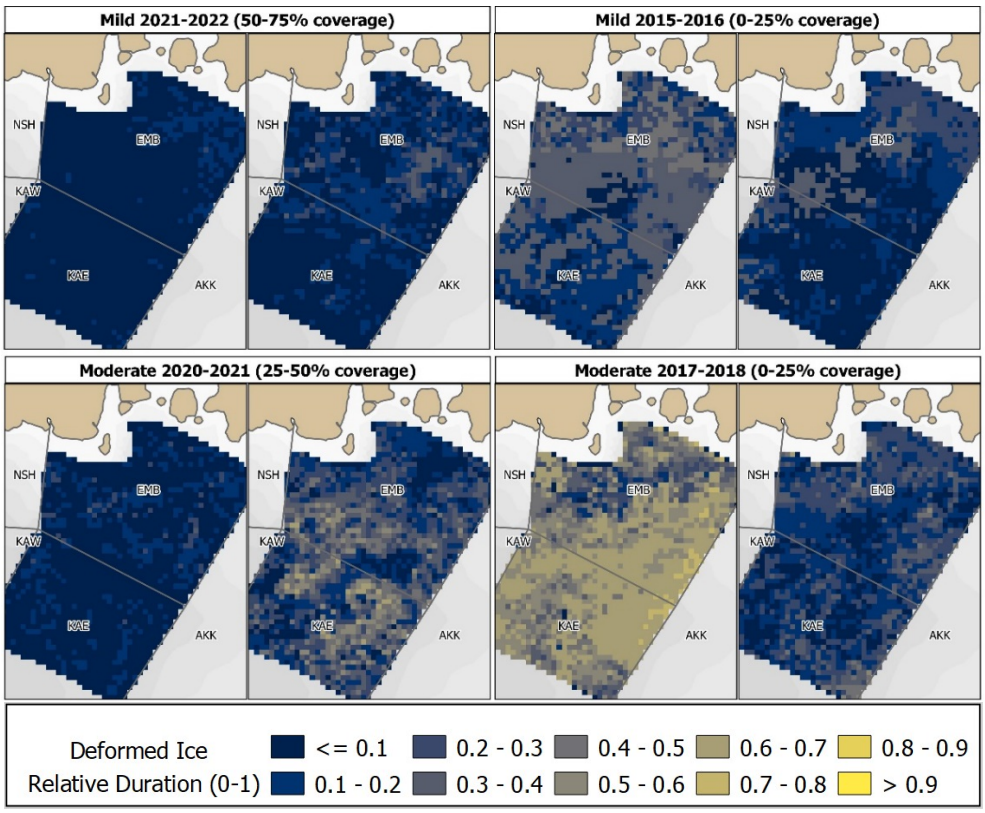

Figure 6 Relative duration of deformed ice occurrence by deformed (left) and semi deformed (right) categories, bins of spatial coverage and season.

Supporting Long-Term Planning and Forecasting

Further classification by season severity that affects the rate of deformation as was observed during analysis of derived data becomes a forecasting tool to plan seasonal operations depending on the degree of ice cover deformation. For example, with known rate of a season severity in the beginning of winter may be a good indication if additional mitigation measures

should be considered by the part of the season when peak of deformed ice coverage is achieved. Figure 7 shows there is a month between December when it is already known whether a season is mild or severe to the end of January and February when peak coverage with deformed ice normally occurs. This is enough lead time to decide for applying addition mitigation measures or abandoning and demobilizing sensitive operations. Most importantly there is spatial differentiation for such forecast that can be a quantified justification why some operations are subject to substantial risk in one part of the area while the same operation may persist with tolerable risk in a different part.

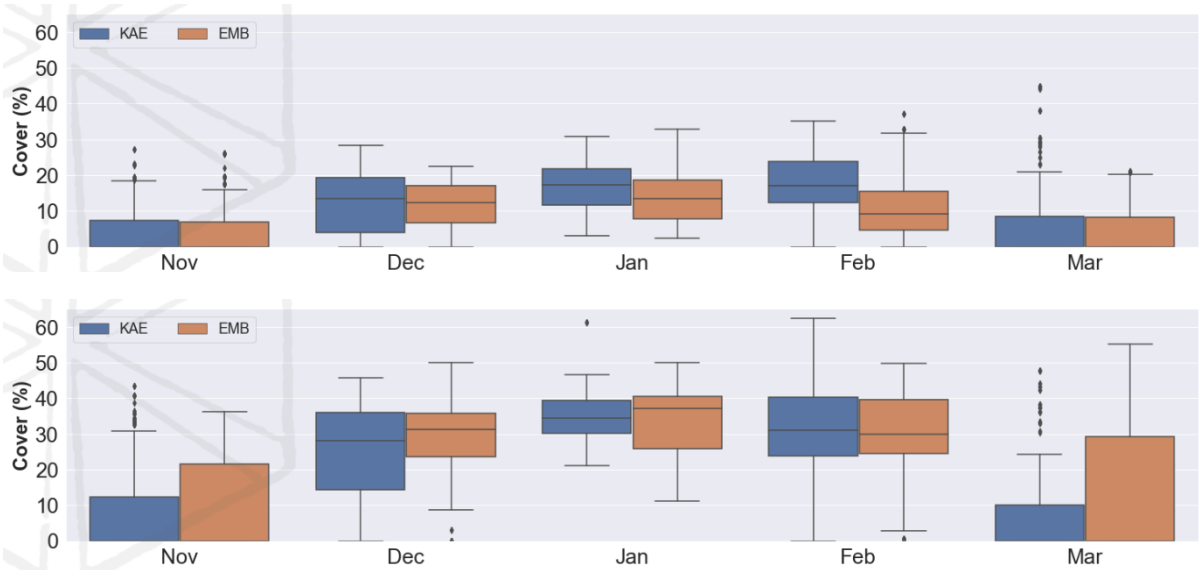

Figure 7 Monthly distribution of deformed (top) and semi deformed (bottom) ice cover for all seasons from 2014 to 2022 in Kashagan East and Emba forecast zones. See Dutoit (2012) for box plot visualization of quartiles.

The above examples are targeted to serve as a tool for planning operations in the near future, be that next month of winter or next season. In addition to this immediate requirement for data driven decision making processes, there are now a lot of queries that arise during the last years to estimate effects of climate change and project impact analysis ten-twenty years ahead and more. Connecting this dataset to climatic indexes observed in the region becomes a solution for such a type of analysis.

Connecting to Climate Indexes

Deformed ice coverage through a season in a certain area depends on several factors. The range of factors starts from sufficient ice thickness to form significant ice rubble or rafted features to cumulative time ice cover was mobile and there were drift events that could lead to deformation of ice cover. Ice thickness in the study area is controlled with Freezing Degree Days (FDD) accumulated during the season due to ice cover being immobile for most moderate and severe seasons. It may be a different situation with higher variation during mostly mobile extremely mild and mild seasons. Nevertheless, FDD is a good reference index for inter-seasonal comparison of effects form ice thickness.

Figure 8 shows seasonal distribution of deformed and semi deformed ice coverage over two zones in the study area binned by FDD accumulated during season when deformation occurred. To remove bias from season duration and to make intensity of the phenomena comparable

between seasons it was set fixed for the period from November 01 to April 15 based on observations from 2014 to 2022. The resulting relationship illustrates the effect of winter severity on ice cover deformation.

Highest deformed ice coverage for both categories was observed during winters with FDD ranging from 500 to 600. Median and lower quartiles (Turney, 2023) of deformed ice coverage being near zero during winters with low FDD below 300 degree-days shows the intensity and frequency of the phenomena (both deformed and semi deformed ice cover) is low over both zones in the area of interest during extremely mild and mild seasons. This can be explained with most season duration being open water that by default means no deformed ice.

The maximum deformed ice coverage is reached during seasons with FDD ranging from 500 to 600 degree-days. The value starts decreasing with higher FDD. This observation is also valuable and explainable. As with higher FDD ice thickness grows thicker and less mobile there are less drift events that lead to ice cover deformation.

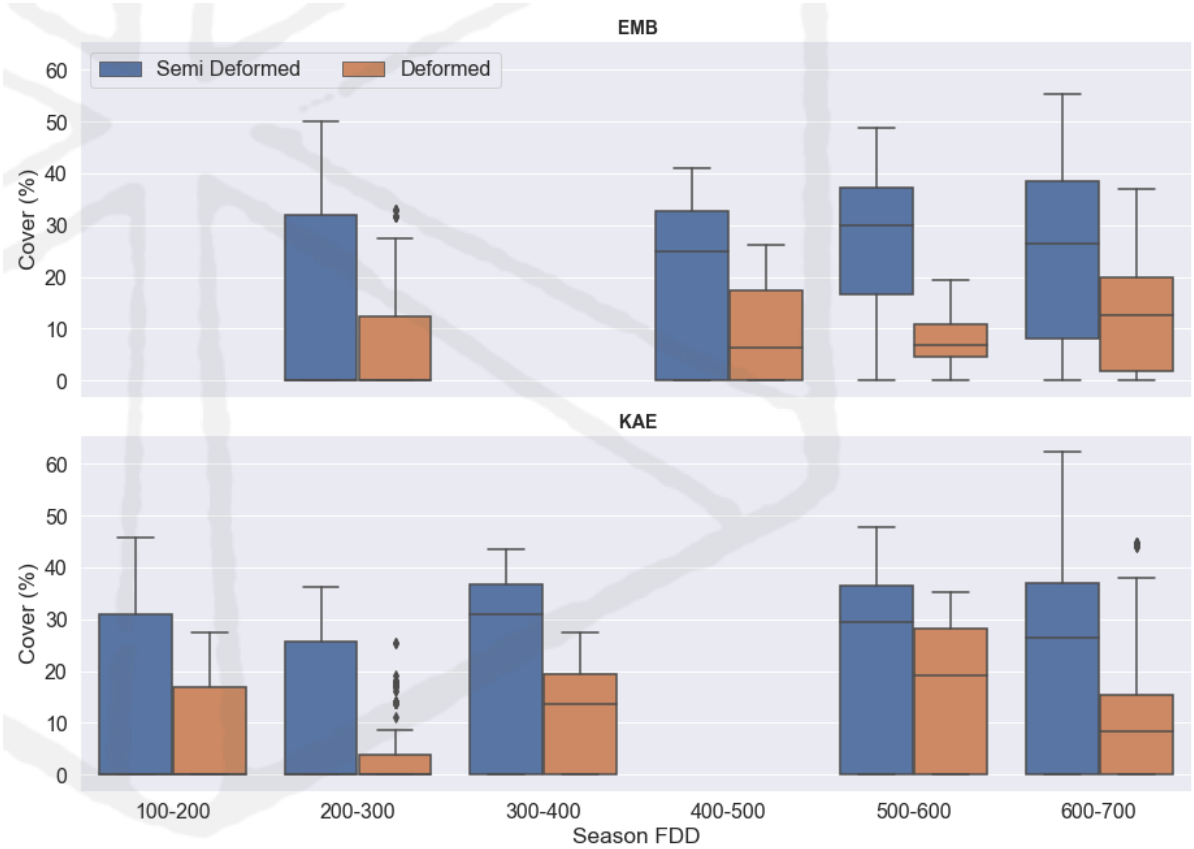

Figure 8 Seasonal (November 01 - April 15) distribution of daily deformed and semi deformed ice coverage over KAE (top) and EMB (bottom) zones versus accumulated FDD for seasons 2014-2022. Median and lower quartiles for 100-300 FDD are near zero. See Dutoit (2012) for box plot visualization of quartiles.

Following the logic and building connection between FDD and deformed ice coverage rates, further projections of air temperature in the region become informative for projections of the phenomena and associated impact assessments. This is the subject of further research for various applications in the region.

More accurate projections can be achieved with reference to Ice Volume records for zones in the areas as it also accounts for drift observations and variation of ice masses due to dynamic processes occurring in the region as discussed by Vernyayev et al. (2023b).

CONCLUSIONS

This approach (k-means clustering and classification of ice cover in SAR images) to identification of deformed ice coverage was found to be an effective data acquisition method. The most important advantage of the method is that human involvement in the analysis is only needed at the first set-up for a specific area while the rest of processing regardless of area and duration is conducted automatically. The best results are achieved in the case of available detailed ice cover classification that compensates for limitation of SAR data interpretation.

The list of practical insights for operations and engineering is yet to be fully disclosed. Although the dataset is limited with good coverage only in time and spatial distribution while vertical component (keel depth and sail height) is not extracted from the satellite image this imperfection is well compensated by regular data structure and geographical reference. With these references it is easy and possible to join spatial data with field measurements to achieve full informativeness of delivered analytics. Experience showed that more added value is achieved with measurements from bottom founded ice profiling systems as they are similarly continuous and consistent.

Our next step to enhance the accuracy of the algorithm is the development of a supervised machine learning algorithm with manually selected best examples of successive detections and misclassifications. This filtering step and dependency on availability of detailed ice cover classification data will be eliminated making it possible to deliver quick ice ridge impact analysis in other regions than Caspian.

ACKNOWLEDGEMENTS

This development was only possible due to Copernicus project (https://www.copernicus.eu/en) as a part of EU space program which provides valuable publicly available data for our work such as images from Sentinel constellations and ERA5 climate weather data. Without such programs our work would not be possible, and their open data approach is highly valued in our group.

REFERENCES

Canadian Ice Service [Online], 2005, Manual of Ice (MANICE), available at: https://www.canada.ca/en/environment-climate-change/services/weather-manuals-documentation/manice-manual-of-ice.html [Accessed 01 March 2023].

Dutoit S. H. C. 2012. *Graphical Exploratory Data Analysis*. Springer.

qEicken, H., Mahoney, A. R., 2015. Sea Ice: Hazards, Risks, and Implications for Disasters. *Coastal and Marine Hazards, Risks, and Disasters*, 381–401. https://doi.org/10.1016/B978-0-12-396483-0.00013-3.

ESA, 2014-2023. Copernicus free access hub. Retrieved from https://scihub.copernicus.eu/dhus [Accessed continuously since 2014].

Lloyd Stuart P., 1982, Least squares quantization in PCM. *Information Theory*, IEEE Transactions on 28.2 (1982): pp. 129-137.

Kadranov Y., Sigitov A., Vernyayev S. 2017, Comparison of satellite imagery based ice drift with wind model for the Caspian Sea. *Proceedings of the 24th International Conference on Port and Ocean Engineering under Arctic Conditions*, June 11-16, Busan, Korea, POAC17.

Kadranov Y., Vernyayev S., Sigitov A. 2023, Marine Units Performance Simulation under changing environment in the Caspian Sea. *Proceedings of the 27th International Conference on Port and Ocean Engineering under Arctic Conditions*, June 12-16, Glasgow, UK, POAC23.

Karvonen, J., 2012. Operational SAR-based sea ice drift monitoring over the Baltic Sea. *Ocean Science*, 8(4), 473–483. https://doi.org/10.5194/OS-8-473-2012.

Linow, S., Hollands, T., & Dierking, W., 2015. An assessment of the reliability of sea-ice motion and deformation retrieval using SAR images. *Annals of Glaciology*, *56*(69), 229–234. https://doi.org/10.3189/2015AOG69A826.

Lohse, J., Doulgeris, A. P., & Dierking W., 2020. Mapping sea-ice types from Sentinel-1 considering the surface-type dependent effect of incidence angle. *Annals of Glaciology*, 61(83), 260–270. https://doi.org/10.1017/AOG.2020.45.

Phillips, O. M., 1988: Radar Returns from the Sea Surface—Bragg Scattering and Breaking Waves. J. Phys. Oceanogr., 18, 1065–1074.

Sandven, S., Johannessen, O.M. 2006. Sea ice monitoring by remote sensing. The American Society for Photogrammetry & Remote Sensing.

Scheuchl, B., Caves, R., Cumming, I., & Staples, G. (2001). Automated sea ice classification using spaceborne polarimetric SAR data. *International Geoscience and Remote Sensing Symposium (IGARSS)*, 7, 3117–3119. https://doi.org/10.1109/IGARSS.2001.978275.

Sigitov A., Kadranov Y., Vernyayev S., 2019, Analysis of Stamukhi Distribution in the Caspian Sea. *Proceedings of the 25th International Conference on Port and Ocean Engineering under Arctic Conditions*, June 9-13, Delft, The Netherlands, POAC19.

Turney, S. 2023, Quartiles & Quantiles | Calculation, Definition & Interpretation. Scribbr. Retrieved March 29, 2023, from https://www.scribbr.com/statistics/quartiles-quantiles/.

Vernyayev S., Kadranov Y., Sigitov A., Vernyayeva I. 2023a Caspian Sea Ice Cover Hindcast Database. *Proceedings of the 27th International Conference on Port and Ocean Engineering under Arctic Conditions*, June 12-16, Glasgow, UK, POAC23.

Vernyayev S., Sigitov, A., Kadranov, Y, Vernyayeva, I. 2023b, Caspian Seasonal Ice Volume Trends in Recent History. *Proceedings of the 27th International Conference on Port and Ocean Engineering under Arctic Conditions.* June 12-16, Glasgow, UK, POAC23.

WMO, 2014, WMO Sea-Ice Nomenclature. World Meteorological Organization. WMO No.259.